

Conductance of a short spin incoherent Hubbard chain; Monte Carlo calculations

Olav F. Syljuåsen¹

¹*NORDITA, Blegdamsvej 17, DK-2100 Copenhagen Ø, Denmark*

(Dated: December 2, 2024)

The DC conductance of a short Hubbard chain coupled to leads is investigated using quantum Monte Carlo. In contrast to the Luttinger liquid regime, where the conductance is equal to the non-interacting value, the spin incoherent regime displays a conductance that decreases rapidly with chain length down to a value of roughly $1.5e^2/h$ for a four site chain followed by a slower decrease for longer chains. We also discuss the resistance contribution from scattering in the contacts.

PACS numbers: 71.10.Pm, 73.23.-b, 71.10.Fd, 73.63.Nm

INTRODUCTION

Interacting electrons in one dimension (1D) do not obey conventional Fermi liquid theory. Instead they form an interacting liquid known as a Luttinger liquid (LL) with separated spin and charge excitations. Perhaps unfortunately, the LL has no signature on the low temperature DC conductance of clean 1D systems, as the DC conductance of a LL coupled to leads is identical to the non-interacting value $2e^2/h$ regardless of the interaction strength[1]. However, there has recently been focus on a less studied regime of 1D electron systems where the LL description does not apply. In this so called spin incoherent regime it has been argued that the DC conductance is reduced to e^2/h , half the non-interacting value[2]. This result has been forwarded as a candidate to explain the conduction anomaly seen at $0.7 \times 2e^2/h$ in very low density quantum point contacts at finite temperatures[3], although no explanation of why the prefactor should be $0.7(\times 2)$ was given. It is the aim of the present study to investigate quantitatively the DC conductance in the spin incoherent regime using numerical simulations of a lattice model system.

At zero temperature, $T = 0$, the low-energy model of a generic interacting 1D electron liquid is the LL which is characterized in part by having independent spin and charge excitations each having separate coupling constants, characteristic velocities and bandwidths. The conductance of a uniform pure LL depends on the charge sector coupling constant K_c alone and is at low temperatures $G = 2K_c e^2/h$ [4, 5]. However this result does not coincide with what is being measured in an experiment where leads are connected to the interacting electron liquid. The leads have a profound influence on the DC conductance and it has been shown by modeling the leads as 1D non-interacting electron gases that the conductance remains at the non-interacting value $2e^2/h$ provided one couples the leads sufficiently smoothly to the interacting wire[1]. Otherwise the conductance is solely determined by scattering in the contacts.

At finite temperatures the magnitude of the bandwidths of the spin and charge excitations become im-

portant. In general the spin bandwidth J is smaller than the charge bandwidth E_f when the interaction energy is bigger than the kinetic energy. Thus a situation where $J \ll T \ll E_f$ is conceivable. This is known as the spin incoherent regime, where in contrast to the LL regime, the electron Green function displays non-propagating spin excitations[6, 7], a broad momentum distribution[8], and an anomalous density of states[9, 10]. The Green function close to a boundary has also been explored[11] as well as Coulomb drag effects[12], the Fermi edge singularity[13] and transport properties in the presence of impurities[14]. It was argued in Ref. [2] that spin-charge separation gets violated when leads are coupled to a spin incoherent wire, and as a consequence the DC conductance is renormalized to a value e^2/h [2]. While the result in Ref. [2] was obtained for an electron liquid at low densities forming a Wigner crystal, it has been argued that the physics of the spin incoherent regime is largely independent of microscopic details, and that one might as well replace the electron gas with a model having short-range interactions like the Hubbard model. This was utilized in Ref. [15] where the non-equilibrium conductance and noise of a spin incoherent chain coupled to leads was calculated in two regimes, a strongly biased regime and with dissipative spin damping, both giving a conductance e^2/h .

The Hubbard model Hamiltonian is

$$H = -t \sum_{\langle ij \rangle, \sigma=\{\uparrow, \downarrow\}} (c_{i\sigma} c_{j\sigma}^\dagger + c_{j\sigma} c_{i\sigma}^\dagger) + \sum_i u_i n_{i\uparrow} n_{i\downarrow} \quad (1)$$

Where $c_{i\sigma}$ is the spin σ fermion annihilation operator at site i , and $n_{i\sigma}$ is the corresponding density operator. In order to model non-interacting leads and smooth contacts the interaction potential u_i is taken to be site-dependent. We treat a 1D lattice with L sites using open boundary conditions and divide it into five regions, see Fig. 1: Two lead regions each of length L_L where $u = 0$, an interacting chain region where $u = U$ and two contact regions each of length L_C where u is site-dependent so that the particle density in the chain region interpolates roughly linearly to the density in the lead. Throughout this Letter we add a uniform chemical potential $\mu = -0.3t$ causing the density in the lead regions to be ~ 0.9 , slightly less than



FIG. 1: The 1D lattice with noninteracting lead regions of length L_L , contact regions of length L_C , and the fully interacting chain of length L_W .

half-filling. The temperature is $T = t/80$ and $L = 192$. To avoid complications due to Kondo physics, we keep L_W even, yet we expect that our results also apply to odd L_W above the Kondo temperature.

For the Hubbard model the bandwidth of the spin excitation spectrum is $J = \frac{4t^2}{U}n(1 - \frac{\sin(2\pi n)}{2\pi n})$, while the bandwidth of the charge spectrum is proportional to the Fermi energy E_f . The spin incoherent regime $J \ll E_f$ is thus realized for low densities, or equivalently for large U . In addition T must be placed in-between these scales. The latter is more demanding for low densities than for large U , because of the smallness of E_f at low densities, thus requiring very low temperatures which are costly using the numerical technique employed here. Therefore we will model a chain in the spin incoherent regime by setting $U = \infty$ in the interacting region. This implies $J = 0$ even for high densities, thus E_f can be kept of the order t .

In order to investigate the 1D inhomogeneous system Eq. (1) we employ the Stochastic Series Expansion (SSE) quantum Monte Carlo method with directed-loop updates[16]. Fermion quantum Monte Carlo simulations frequently come with a minus-sign problem. However this is avoided in 1D using open boundary conditions. The fermions are represented in the occupation number formalism following the sign convention described in Ref. [17], and the directed-loop rules were taken from Ref. [18]. In addition to having updates that add/remove a particle with a certain spin we also employ moves that flips the spin of a particle. This is necessary to ensure short autocorrelation times in the spin incoherent regime.

The DC conductance G is evaluated as the linear response of the current operator j at position x to a discontinuity in the chemical potential at y in the limit of zero frequency

$$G = \lim_{z \rightarrow 0} g(z),$$

$$g(z) = \text{Re} \frac{i}{\hbar} \int_0^\infty dt e^{izt} \langle [j_x(t), P_y] \rangle$$

where P_y is the sum of fermion charge density operators at sites to the right of y , $P_y = e \sum_{y' > y} n_{y'}$. The extrapolation to zero frequency can be taken along any path in the complex plane. We will extrapolate along the imaginary axis[19], thus z is taken to be imaginary and is denoted $z = i\omega$. Using the charge/current continuity relation for a 1D system with open boundary conditions one finds that $g(i\omega)$ can be evaluated at the Matsubara

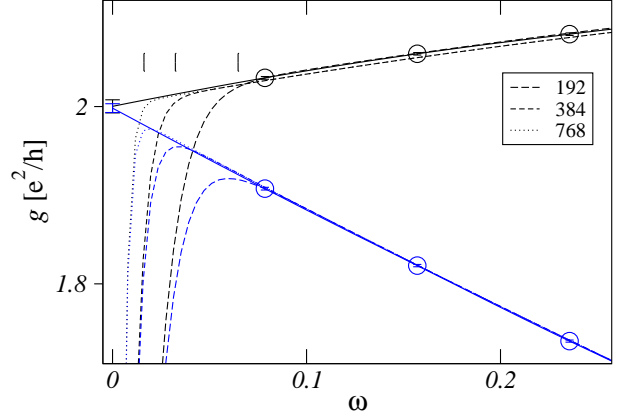


FIG. 2: (Color online) Imaginary frequency conductance for free fermions. The dotted, dashed and long dashed lines are exact results for different system sizes L indicated by the legends. The circles are Monte Carlo data at the three lowest non-zero Matsubara frequencies for $L = 192$. The solid lines are the extrapolated Monte Carlo results using the prescription in the text and the error bars at $\omega = 0$ indicate the DC conductance in the thermodynamic limit. The upper set of curves (black) is for $x = y = L/2 - 1$ and the lower (blue) is for $x = L/2 - 1$, $y = x + 1$. The three vertical bars indicate the frequency $\omega = 2\pi\hbar v_f/L$ for the three system sizes $L = 768, 384, 192$.

frequencies $\omega = \omega_n \equiv 2\pi n T$ as[20]

$$g(i\omega_n) = \frac{\omega_n}{\hbar} \int_0^{\beta\hbar} d\tau \cos(\omega_n\tau) \langle P_x(\tau) P_y(0) \rangle. \quad (2)$$

This correlation function which involves only density operators is easily evaluated using the Monte Carlo method. While for a finite system, $g(i\omega = 0) = 0$, the correct way of obtaining the conductance in the thermodynamic limit is to first take the infinite system size limit and then extrapolate to zero frequency. For a big enough system the finite Matsubara frequencies is not appreciably affected by the system size, thus the DC conductance in the thermodynamic limit can be gotten from extrapolating the conductance at the finite Matsubara frequencies to zero along the imaginary frequency axis. We do this by constructing the minimal order (diagonal) rational polynomial function coinciding with the Monte Carlo data and take its value at $\omega = 0$.

Fig. 2 shows how the extrapolation to zero frequency is carried out for free fermions. The two set of curves are for different choices y and x of where the potential discontinuity is applied and its response is measured. Both choices lead to the same extrapolated value which is consistent with the exact value $G = 2e^2/h$. The circles indicate the Monte Carlo data and the solid lines are the extrapolations. The dashed and dotted curves that approach 0 for low ω are exact results on chains of different lengths. They start to deviate

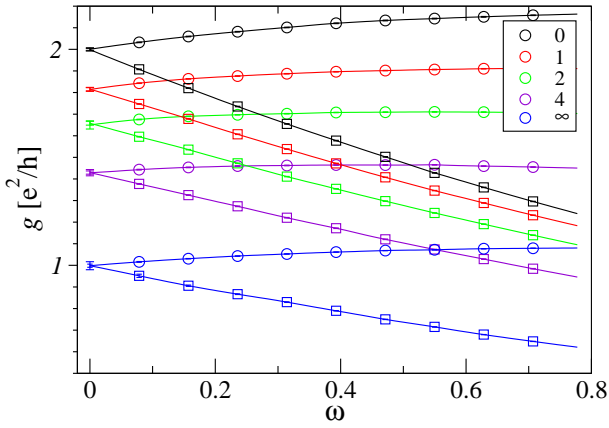


FIG. 3: (Color online) Imaginary frequency conductance extrapolated to zero frequency for uniform Hubbard chains with different values of U . From top to bottom $U/t = 0, 1, 2, 4, \infty$. $x = L/2 - 1$. The circles are for $y = x$ and the squares are for $y = x + 1$.

from the extrapolated results at $\omega \approx \hbar v_f 2\pi/L$ which correspond to frequencies lower than the level spacing of the system. This sets a lower limit, $L > \hbar v_f \beta$, for the system size needed at a finite temperature $T = 1/\beta$, in order to ensure that the finite Matsubara frequencies all reflect the infinite size limit.

To check our method we obtain first the DC conductances for uniform chains with no leads having different values of the interaction U . The measured particle densities are 0.903, 0.781, 0.696, 0.601, 0.457 for $U/t = 0, 1, 2, 4, \infty$ respectively. Fig. 3 shows the results containing two different extrapolations for each value of U . Taking the average of the extrapolated results we obtain $G/(e^2/h) = 1.999 \pm 0.004, 1.815 \pm 0.006, 1.654 \pm 0.010, 1.429 \pm 0.008, 0.998 \pm 0.014$ for $U/t = 0, 1, 2, 4, \infty$ respectively. These values agree well with $G = 2K_c e^2/h$, where K_c is the Luttinger liquid charge sector coupling constant which value can be obtained for the Hubbard model for a given density and U by the Bethe Ansatz[21].

We now attach leads to the $U = 4$ Hubbard chain. Fig. 4 upper panel shows the imaginary frequency conductance and its extrapolation to zero frequency for different lengths L_W of the interacting region. In order to make the contact resistance small we have made contact regions of length $L_C = 2$. While at high Matsubara frequencies the conductance curves are close to the conductance curve of the uniform chain there is a change in behavior when the frequency gets below $\omega \sim \hbar v_f / L_W$, where the conductance curves extrapolate towards the non-interacting value in accordance with Refs. [1]. To see how the value of the DC conductance depends on the length of the contact regions we show in Fig. 4 lower panel the conductance for different lengths of the contact regions keeping the length of the interacting chain fixed.

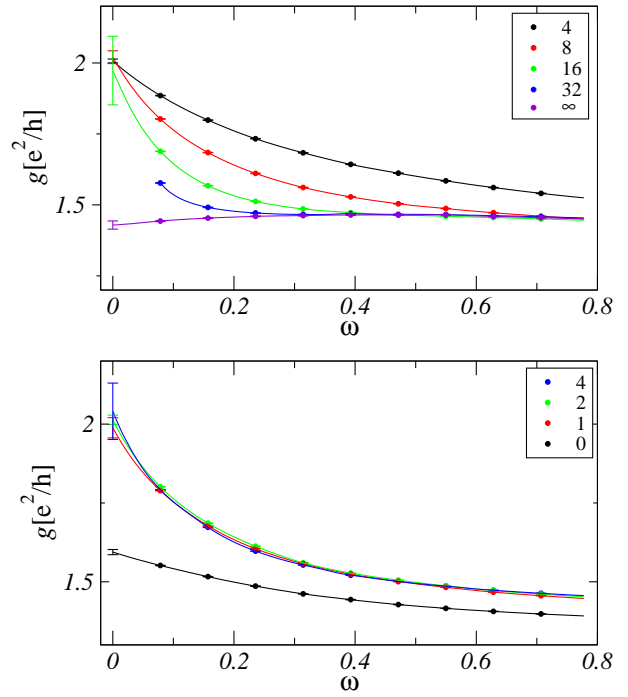


FIG. 4: (Color online) Imaginary frequency conductance for an interacting ($U = 4t$) chain with leads. Upper panel: The curves are for different L_W indicated by the legends and a fixed $L_C = 2$. For comparison the uniform(∞) $U = 4t$ chain without leads is also shown (lowest curve). Lower panel: The curves are for different L_C indicated by the legends and a fixed $L_W = 8$. In both panels $x = y = L/2 - 1$.

The curve with an abrupt contact region ($L_C = 0$) shows a lower DC conductance than the others which appear to have reached the adiabatic limit already for $L_C = 1$.

To reach the spin incoherent limit we set $U = \infty$. In the simulations this is achieved by restricting the Hilbert space so that no sites in the interacting region can be doubly occupied. Fig. 5 upper panel shows the imaginary frequency conductance and its extrapolation for spin incoherent chains of different lengths coupled to leads. As in the LL regime, the data at low imaginary frequency differ from that of the uniform chain(labeled ∞) and extrapolate to values larger than e^2/h . We have not shown the extrapolation for the longest chains due to the fact that only the few lowest Matsubara frequencies distinguish these curves from the uniform one causing excessively large error bars. Nevertheless it is quite clear that the DC conductances of the longest chains also extrapolate to values larger than e^2/h . This is rather remarkable in view of the exponential decrease of the single-particle Green function in the spin incoherent regime. The extrapolated DC conductances are plotted in the inset and reveal a rapid decrease with increasing chain length to a value $\sim 1.5e^2/h$ for $L_W = 4$, and then a further slower decrease. Note that this intermediate conductance value is close to the value relevant to explain the 0.7 anomaly

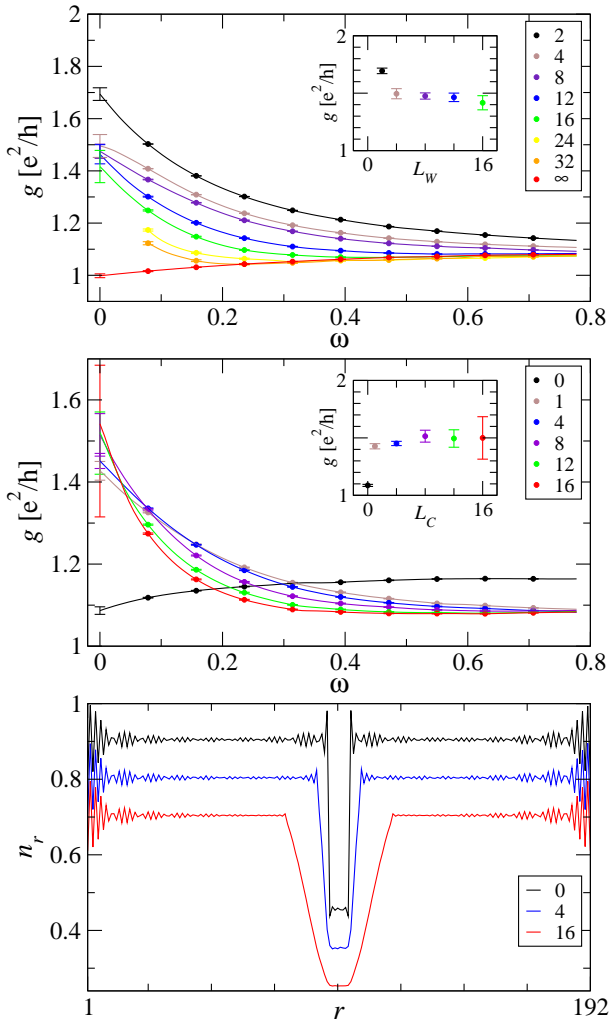


FIG. 5: (Color online) Imaginary frequency conductance of a spin incoherent chain with leads. $y = x = L/2 - 1$. a) curves are for different L_W indicated by the legends, $L_C = 2$. The inset shows the DC conductances. b) Fixed $L_W = 8$ and different L_C indicated by legends. Inset: DC conductances. c) particle density vs. site for different L_C . $L_W = 8$. The $L_C = 4(16)$ curve has been shifted downwards by 0.1(0.2) for clarity.

in quantum point contacts.

In addition to the intrinsic resistance of the interacting region, our results include possible contributions from scattering in the contact regions. The contact regions used were of length $L_C = 2$, which is long enough to give adiabatic contacts in the LL regime, see Fig. 4. However, in order to investigate the role of the contacts we show in Fig. 5 middle panel results for different sizes of the contact regions. While there is a significant resistance contribution for abrupt junctions, $L_C = 0$, there are only small differences between the DC conductances for contacts of lengths $L_C \geq 1$, see inset. It is not entirely clear however, due to the large error bars for the largest values of L_C , if the DC conductance has saturated or

will keep increasing for even larger L_C 's. Assuming saturation we estimate that the contact contribution to the reduced conductance is $\sim 0.1e^2/h$ for $L_C = 2$. The density variations in the contacts causing scattering is shown in Fig. 5. Note the rather abrupt density changes that causes resistance in the case $L_C = 0$, compared to the smooth density variations for $L_C = 16$.

Our results shows that the DC conductance decreases slowly with chain length L_W for $L_W > 4$. It is however unclear as to what sets the rather long length scale associated with this slow decrease. It is plausible that this is related to the magnitude of terms in the effective Hamiltonian breaking spin-charge separation. It also remains to be seen to which extent the results reported here are universal.

The simulations were in part carried out using computers provided by the University of Aalborg, Denmark and the University of Tartu, Estonia using the NorduGrid ARC middleware.

[1] D. L. Maslov and M. Stone, Phys. Rev. B **52**, R5539 (1995); V. V. Ponomarenko, Phys. Rev. B **52**, R8666 (1995); I. Safi and H. J. Schulz, Phys. Rev. B **52**, R17040 (1995).
[2] K. A. Matveev, Phys. Rev. Lett. **92**, 106801 (2004); Phys. Rev. B **70**, 245319 (2004).
[3] K. J. Thomas *et al.*, Phys. Rev. Lett. **77**, 135 (1996).
[4] W. Apel and T. M. Rice, Phys. Rev. B **26**, 7063 (1982).
[5] C. L. Kane and M. P. A. Fisher, Pjys. Rev. Lett. **68**, 1220 (1992).
[6] V. V. Cheianov and M. B. Zvonarev, Phys. Rev. Lett. **92**, 176401 (2004); V. V. Cheianov and M. B. Zvonarev, J. Phys. A **37**, 2261 (2004).
[7] G. A. Fiete and L. Balents, Phys. Rev. Lett. **93**, 226401 (2004).
[8] V. V. Cheianov, H. Smith, and M. B. Zvonarev, Phys. Rev. A **71** 033610 (2005).
[9] G. A. Fiete, J. Qian, Y. Tserkovnyak and B. I. Halperin, Phys. Rev. B **72**, 045315 (2005).
[10] K. A. Matveev, A. Furusaki, and L. I. Glazman, cond-mat/0605308
[11] P. Kakashvili and H. Johannesson, cond-mat/0605062.
[12] G. A. Fiete, K. Le Hur, and L. Balents, Phys. Rev. B **73**, 165104 (2006)
[13] G. A. Fiete, cond-mat/0605101
[14] G. A. Fiete, K. Le Hur and L. Balents, Phys. Rev. B **72**, 125416 (2005).
[15] M. Kindermann and P. W. Brouwer, cond-mat/0506455.
[16] A. W. Sandvik and J. Kurkijärvi, Phys. Rev. B **43**, 5950 (1991); O. F. Syljuåsen and A. W. Sandvik, Phys. Rev. E **66**, 046701 (2002).
[17] A. W. Sandvik, Jour. Phys. A **25**, 3667 (1992).
[18] O. F. Syljuåsen, Phys. Rev. E **67**, 046701 (2003).
[19] S. Kirchner, H. G. Evertz, and W. Hanke, Phys. Rev. B **59**, 1825 (1999).
[20] K. Louis and C. Gros, Phys. Rev. B **68**, 184424 (2003).
[21] H. J. Schulz, Phys. Rev. Lett. **64**, 2831 (1990).